Sādhanā (2020)45:288
https://doi.org/10.1007/s12046-020-01519-7

A novel non-customary method of image compression based on image spectrum

HIMANSHU KUMAR[1,*], SUMANA GUPTA[2] and K S VENKATESH[2]

[1]Department of Electrical Engineering, IIT Jodhpur, Jodhpur, India
[2]Department of Electrical Engineering, IIT Kanpur, Kanpur, India
e-mail: hkumar@iitj.ac.in; sumana@iitk.ac.in; venkats@iitk.ac.in

MS received 5 October 2018; revised 2 September 2020; accepted 13 September 2020

Abstract. Compression of multimedia content is an important processing step and backbone of real life applications in terms of optimum resource utilization in transmission and storage. It is an established field of research with very little scope for further improvement in achieved compression through customary coding-based compression techniques. Consequently, non-customary compression methods have become an important area for future research. Based on the principle 'Any information that can be restored can be compressed', we propose a novel spectrum-based image compression technique to further reduce the data footprint with satisfactory quality metric for images. We first blur the image with a point spread function (PSF) determined using frequency content of the given image. Blurring increases the DC component in the image, which in turn gets further compressed compared with original image by DCT-based JPEG compression. To recover the image, we perform deconvolution using the known blur PSF. Results obtained show further improvement of $20-30\%$ in achieved compression with respect to original JPEG compressed image with satisfactory quality of recovered image.

Keywords. Image compression; spectrum; zero preservation; deconvolution; deblurring.

1. Introduction

Compression is an important and established field of research in the area of image and video processing. Rapid increases of various devices and technologies pose a serious question on storage and transmission of existing multimedia content between various sources and destinations. Compression enables us to address these challenges by providing efficient storage and transmission of multimedia content.

In this area of research, focus has been on coding the content efficiently based on resolution of devices, resources and human perception. Thus the aim of compression is to remove the various redundancies present in data, viz coding redundancy [1–3], pixel-correlation redundancy [4, 5] and perceptual redundancy [6–8]. Compression methods focusing on reducing coding and pixel-correlation redundancy are lossless, while methods that focus on reducing the perceptual redundancy are lossy.

State of the art methods use a combination of these techniques to achieve the optimum compression; for example, efficient coding such as Huffman coding [1] is used to reduce coding redundancy after any encoding that reduces the data footprints (pixel-correlation redundancy). In such aspects, the scope for significant improvement over present techniques in terms of achieved compression using coding and perceptual redundancy is very little. However, pixel-correlation redundancy offers a range of possibilities of significant improvement in achieved compression. We refer to these methods as non-customary methods of compression, e.g., super-resolution from underlying pattern in low-resolution image to restore the original image to achieve compression as in Google's RAISR [5]. Methods such as those in [9, 10] and [11] use transform domains such as wavelets to encode the data. These methods are very sensitive to noise and work well in specific cases only.

All the non-customary methods of compression are complementary to each other rather than competing. JPEG compression, which is a combination of DCT-based compression and Huffman coding, is an example of such a method. Thus, they can be applied one after the other. This creates a framework for applying various compression schemes at once to an input image. In this paper, we present a novel spectrum-based image compression method. This work is an extension of [12] and includes further detailed experiments to validate the proposed method.

The remainder of the paper is organized as follows. Section 2 discusses the previous and ongoing research in the field of image compression. Section 3 presents the proposed spectrum-based image compression method. We

*For correspondence
Published online: 19 November 2020

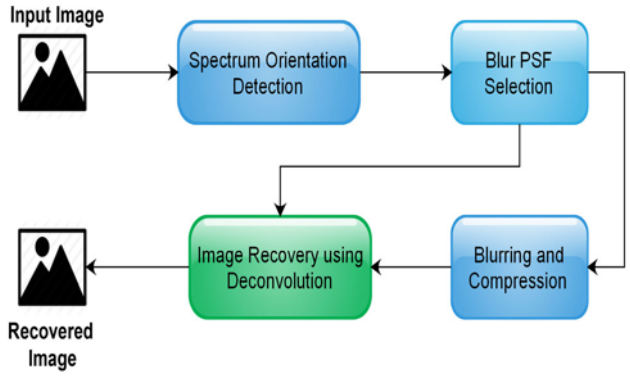

Figure 1. Flow diagram for the proposed spectrum-based compression method.

discuss the design and details of the proposed method in section 4. In section 5, we present the results for the proposed compression method. Discussion, limitations and conclusions are provided in sections 6, 7 and 8, respectively.

2. Previous works

The principle of compression is 'any information that can be restored can be compressed'. Many methods/coding schemes exist in literature that employ different information such as colour coding, motion information and human visual perception to compress the images/videos.

Huffman [1] proposed an efficient lossless coding scheme for optimum use of number of bits to reduce the data trace. However, further compression can be achieved by correlating the data since images are collection of highly correlated data. Methods in [2] and [3] used different transform domains to encode the image information to achieve compression. These methods focus on reducing coding redundancy with very little scope for further significant improvement in achieved compression.

Wallace [6] introduced compression and coding standard JPEG for images on the basis of perceptual measure. In this technique, image contents imperceptible to human vision system are removed to achieve compression. It is a lossy compression algorithm and utilizes discrete cosine transform (DCT) such that perceptually there is no observable difference in image quality. Similarly, methods in [7] and [8] use different transform domains to apply the perceptual measure to discard less significant coefficients to attain the compression. These methods remove perceptual redundancy in data using various domain transformations. However, such a strategy too has very little scope for further significant improvement in achieved compression.

Barreto *et al* [4] used patch-based super-resolution to compress the image. A downsampled image is used in place of full size image to reduce the data trace for transmission. The transmitted downsampled image is upsampled and refined using super-resolution to attain good quality image. Dong *et al* [14] used deep convolutional network for super-resolving the image. Romano *et al* [5] at Google proposed RAISR for attaining good quality super-resolved image using machine learning. Here, transmitted downsampled image is upsampled using RAISR to attain good quality image. Methods such as those in [15, 16] and [17] encode full images based on recurrent pattern using neural network to attain the compression.

Zhang [18] used pseudorandom permutation to encrypt an original image and later compressed it by discarding the excessively rough and fine information of coefficients generated from orthogonal transform. The image is reconstructed iteratively with the help of spatial correlation in natural image. However, this technique requires large processing time and the notion of spatial correlation prior may not be true in general. Akhtar *et al* [19] used simple addition-based smoothing and quantization techniques in 4×4 blocks to attain the compression. However, they obtained compression metric comparable to that of JPEG compression.

State of the art methods such as [20–22] and [23] encode colour information in a single channel by hiding information as textured content or as a sparse representation. This minimizes the footprint of data and results in compression. In principle, different classes of methods can be applied simultaneously to achieve compression. However, applying methods of one class alters the data and assumed priors/trained model may no longer hold true; for example transforming colour image to single-channel image may alter the texture regions and trained model for super-resolution will fail due to change in texture region. These methods employ pixel-correlation to achieve compression and have a lot of scope for further significant improvement in achieved compression.

In this paper we propose a spectrum-based image compression method, which can be used along with existing customary and non-customary methods of compression. The proposed method compresses the image by blurring it with appropriate blur point spread function (PSF) followed by JPEG compression. Blurred image is restored at the receiving end via deconvolution using known blur PSF. This process reduces the data footprint and results in compression. The main contributions made in this paper are the following:

- Introduction of image spectrum prior for natural images, which states that the spectra of natural images orient in vertical direction. This subsequently helps in reducing the computation time in PSF selection.
- A robust PSF selection algorithm for image blurring and recovery.
- A method to relate the parameters of various PSFs, which govern spread of the PSF, e.g. blur length L of motion blur and σ of Gaussian blur.

- A novel spectrum-based image compression technique that can be utilized along with other existing compression methods.
- Validation of the proposed method over a large database.

3. Proposed method

In this section, we describe the architecture of the proposed spectrum-based image compression scheme shown in Figure (1). The proposed compression method is a combination of two strategies, viz removal of pixel-correlation redundancy and perceptual redundancy. We increase the correlations among pixels by introducing blurring with known PSF in the direction of maximum frequency content occurrence before compression.

The following outline describes the proposed compression method shown in Figure (1).

- We first estimate the orientation for the blurring PSF from the spectrum of given image.
- Using this estimated orientation, we select the blurring PSF.
- We then blur the image with selected PSF and compress the blurred output using standard JPEG scheme having parameter quality as 75% and bit depth as 8.
- Finally, we recover the original image by deblurring the compressed image using the selected PSF.

Detailed discussions of the various steps involved in the proposed compression scheme are given in the subsequent sections.

4. PSF selection and compression

Selection of blurring PSF is a crucial step in the proposed compression scheme. In this section, we discuss various aspects of blurring PSF selection.

4.1 *Spectrum orientation detection*

The spectrum of an image contains information about its frequency content. Blurring the image with selected PSF decreases the variation of AC component, which results in more compact coding of image using DCT. This results in better compression compared with original encoded format. Blurring in the direction of maximum frequency content will maximize the correlation between the pixels in the image. This will result in maximum compression for a given PSF when pixel-correlation redundancy-based compression method is applied. We use spectrum orientation to determine the orientation of maximum frequency content, and hence direction of blurring PSF. We apply logarithm operation on the magnitude of Fourier transform $\mathcal{F}$ for calculating the spectrum S of the image I as given in Equation (1):

$$S = \log(|\mathcal{F}(I)|) \tag{1}$$

Later, the orientation $\angle S$ of image spectrum S is taken as the direction of high energy content of the spectrum. Firstly, we generate a mask for the high energy content of the spectrum S as in (2) and apply the morphological operations to refine the mask. Then, we determine the orientation of image spectrum from the eccentricity and orientation of the mask region. In case eccentricity value e is less than 0.7, the spectrum is considered as direction invariant (DI); in other cases, estimated orientation of the mask is taken as the orientation of the image spectrum. This orientation $\angle S$ represents the direction of dominant contents present in the image, e.g. dominant vertical direction of the image spectrum implies that the image contains high amount of horizontally oriented edges, texture, etc.:

$$\angle S = \angle(S > \max(\frac{S}{2})) \tag{2}$$

Figure 2 shows an example of image spectrum and corresponding generated mask. For blur PSF selection, we quantize the orientation in three categories: 0°, 90° and DI. Orientations in $[90° - 20°, 90° + 20°]$ range are quantized as 90°, while orientations in $[0°, 0° + 20°]$ or $[180° - 20°, 180°]$ ranges are quantized as 0°. All other orientations are categorized as DI. More discussion about orientation quantization is given in section 6.

4.2 *Blur PSF selection*

Selection of an appropriate PSF for a given image is a crucial step in our approach. To attain higher deconvolution accuracy, we use 1D blur PSF. However, in general, as image spectrum is not isotropic, the direction of the selected PSF affects the amount of achieved compression. To attain maximum compression, we choose direction of PSF f to be the same as dominant orientation of image spectrum S as given in (2).

However the nature of PSF f may also vary, e.g. Gaussian, Uniform, Triangular, etc. To find optimal blur PSF, we compare various measures such as SSIM, PSNR and

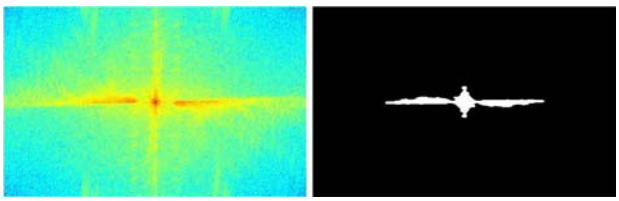

Figure 2. Image spectrum and corresponding mask.

attained compression using these PSFs. However, different PSFs have different parameters and cannot be compared. Hence, to compare various blur PSFs, we introduce and derive notion of equivalent parameter as follows. In this work, we assume that all the given PSFs $f(x)$ belong to $L^2(\mathbb{R})$ and blur parameter σ of Gaussian PSF, blur length L of motion blur and triangular blur PSFs are strictly positive, i.e. $L, \sigma > 0$.

Claim 1 *Any given PSF f(x) can be represented as a closest equivalent Gaussian PSF in $L^2(\mathbb{R})$ with parameter $\hat{\sigma}$ by solving*

$$\hat{\sigma} = \frac{1}{4\int_{-\infty}^{\infty} f(\sqrt{2}\hat{\sigma}y)e^{-y^2}(1-2y^2)dy}.$$

Proof The error E between the equivalent Gaussian PSF and given PSF $f(x)$ in L^2 sense can be written as

$$E = \int_{-\infty}^{\infty}\left(\frac{1}{\sqrt{2\pi\sigma^2}}e^{-\frac{x^2}{2\sigma^2}} - f(x)\right)^2 dx.$$

The closest equivalent Gaussian kernel corresponding to PSF $f(x)$ can be obtained by minimizing the error E with respect to Gaussian kernel parameter σ:

$$\begin{aligned}
\hat{\sigma} &= arg\,min_{\sigma} E \\
&= arg\,min_{\sigma}\int_{-\infty}^{\infty}\left(\frac{1}{\sqrt{2\pi\sigma^2}}e^{-\frac{x^2}{2\sigma^2}} - f(x)\right)^2 dx \\
\frac{\partial E}{\partial \sigma} &= 0 \\
\frac{\partial E}{\partial \sigma} &= \frac{\partial}{\partial \sigma}\int_{-\infty}^{\infty}\left(\frac{1}{\sqrt{2\pi\sigma^2}}e^{-\frac{x^2}{2\sigma^2}} - f(x)\right)^2 dx.
\end{aligned}$$

On applying the differential rule for integration

$$\begin{aligned}
&= \int_{-\infty}^{\infty}\frac{\partial}{\partial\sigma}\left(\frac{1}{\sqrt{2\pi\sigma^2}}e^{-\frac{x^2}{2\sigma^2}} - f(x)\right)^2 dx \\
&= \int_{-\infty}^{\infty} 2\left(\frac{e^{-\frac{x^2}{2\sigma^2}}}{\sqrt{2\pi\sigma^2}} - f(x)\right)\left(\frac{\partial}{\partial\sigma}\left(\frac{e^{-\frac{x^2}{2\sigma^2}}}{\sqrt{2\pi\sigma^2}}\right) - 0\right)dx \\
&= \int_{-\infty}^{\infty} 2\left(\frac{e^{-\frac{x^2}{2\sigma^2}}}{\sqrt{2\pi\sigma^2}} - f(x)\right)\left(\frac{e^{-\frac{x^2}{2\sigma^2}}}{\sqrt{2\pi\sigma^2}}\left(\frac{-1}{\sigma} + \frac{x^2}{\sigma^3}\right)\right)dx \\
&= \underbrace{\int_{-\infty}^{\infty}\frac{2}{\sigma}\left(\frac{e^{-\frac{x^2}{2\sigma^2}}}{\sqrt{2\pi\sigma^2}}\right)\left(\frac{e^{-\frac{x^2}{2\sigma^2}}}{\sqrt{2\pi\sigma^2}}\right)\left(\frac{x^2}{\sigma^2} - 1\right)dx}_{\mathbf{T_1}} \\
&\quad - \underbrace{\int_{-\infty}^{\infty}\frac{2}{\sigma}(f(x))\left(\frac{e^{-\frac{x^2}{2\sigma^2}}}{\sqrt{2\pi\sigma^2}}\right)\left(\frac{x^2}{\sigma^2} - 1\right)dx.}_{\mathbf{T_2}}
\end{aligned} \tag{3}$$

Now consider term $\mathbf{T_1}$ from (3):

$$\begin{aligned}
\mathbf{T_1} &\triangleq \int_{-\infty}^{\infty}\frac{2}{\sigma}\left(\frac{1}{2\pi\sigma^2}e^{-\frac{2x^2}{2\sigma^2}}\right)\left(\frac{x^2}{\sigma^2} - 1\right)dx \\
&= \frac{2}{\sigma}\frac{1}{\sqrt{4\pi\sigma^2}}\int_{-\infty}^{\infty}\left(\frac{e^{-\frac{x^2}{\sigma^2}}}{\sqrt{\pi\sigma^2}}\frac{x^2}{\sigma^2} - \frac{e^{-\frac{x^2}{\sigma^2}}}{\sqrt{\pi\sigma^2}}\right)dx \\
&= \frac{2}{\sigma}\frac{1}{\sqrt{4\pi\sigma^2}}\left(\frac{\sigma^2}{2\sigma^2} - 1\right) = \frac{2}{\sigma}\frac{-1}{4\sqrt{\pi\sigma^2}}.
\end{aligned} \tag{4}$$

Consider term $\mathbf{T_2}$ from (3):

$$\begin{aligned}
\mathbf{T_2} &\triangleq \int_{-\infty}^{\infty}\frac{2}{\sigma}f(x)\left(\frac{1}{\sqrt{2\pi\sigma^2}}e^{-\frac{x^2}{2\sigma^2}}\right)\left(\frac{x^2}{\sigma^2} - 1\right)dx. \\
&\text{Substituting } \frac{x}{\sqrt{2}\sigma} = y \\
\mathbf{T_2} &=
\end{aligned} \tag{5}$$

Now substituting values of $\mathbf{T_1}$ and $\mathbf{T_2}$ obtained from (4) and (5) in (3), we obtain

$$\begin{aligned}
\frac{\partial E}{\partial \sigma} &= \frac{-1}{2\sqrt{\pi\sigma^4}} - \frac{2}{\sqrt{\pi\sigma^2}}\int_{-\infty}^{\infty} f(\sqrt{2}\sigma y)e^{-y^2}(2y^2-1)dy, \\
\frac{\partial E}{\partial \sigma} &= 0 \Rightarrow \hat{\sigma} = \frac{1}{4\int_{-\infty}^{\infty} f(\sqrt{2}\sigma y)e^{-y^2}(1-2y^2)dy}.
\end{aligned} \tag{6}$$

□

As motion blur and triangular blur are most common, we derive the relationships between the blur parameters L of these PSFs and that of the blur parameter σ of the equivalent Gaussian representation. Figure (3) shows examples of motion blur and triangular blur PSFs.

Theorem 1 *Motion blur length L and blur parameter σ for equivalent Gaussian PSF follow a linear relation passing through origin given by (7):*

$$\sigma = cL \qquad \text{where } c \text{ is a constant} \tag{7}$$

Proof We repeat the calculation in Claim (1) with $f(x) := \frac{1}{L}\mathbb{1}_{[\frac{-L}{2},\frac{L}{2}]}$ and obtain (8):

$$\hat{\sigma} = \frac{L}{8\int_0^{\frac{L}{2\sqrt{2}\sigma}} e^{-y^2}(1-2y^2)dy}. \tag{8}$$

From (8), we deduce that $\hat{\sigma}$ is optimal blur length 1 iff $\hat{\sigma}$ satisfies

$$1 = \frac{\hat{\sigma}}{1}\int_0^{\frac{1}{\hat{\sigma}2\sqrt{2}}} 8e^{-y^2}\left(1-2y^2\right)dy$$

and therefore for any $L > 0$

$$1 = \frac{L\hat{\sigma}}{L}\int_0^{\frac{L}{L\hat{\sigma}2\sqrt{2}}} 8e^{-y^2}(1-2y^2)dy.$$

Hence, (8) proves that $L\hat{\sigma}$ is optimal for blur length L. Thus, $\hat{\sigma}$ in (8) evolves linearly with blur length $L > 0$. □

Here, c takes the value 0.35 as determined experimentally. It can also be derived numerically by solving the Transcendental Equation (8).

Theorem 2 Triangular blur PSF with length L and blur parameter σ for equivalent Gaussian PSF follows a linear relation passing through origin as in (10):

$$\sigma = kL \qquad \text{where } k \text{ is a constant.} \tag{9}$$

Proof We repeat the calculation in Theorem (1) with $f(x) := \frac{2}{L}(1 - \frac{2|x|}{L})\mathbb{1}[\frac{-L}{2}, \frac{L}{2}]$ and obtain (10):

$$\hat{\sigma} = \frac{1}{8\int_0^{\frac{L}{2\sqrt{2}\sigma}} \frac{2}{L}\left(1 - \frac{2\sqrt{2}\hat{\sigma}y}{L}\right)e^{-y^2}(1 - 2y^2)dy}. \tag{10}$$

From (10), we deduce that $\hat{\sigma}$ is optimal blur length 1 iff $\hat{\sigma}$ satisfies

$$1 = \frac{\hat{\sigma}}{1}\int_0^{\frac{1}{\hat{\sigma}2\sqrt{2}}} 16\left(1 - 2\sqrt{2}\hat{\sigma}y\right)e^{-y^2}\left(1 - 2y^2\right)dy.$$

Now, proceeding as in Theorem (1), we obtain

$$\sigma = kL \qquad \text{where } k \text{ is a constant.}$$

□

Constant k takes the value 0.2183 determined experimentally as well as using Transcendental Equation (10) for the triangular blur PSF. Theorems (1) and (2) prove that the underlying parameters of the PSFs have linear relationship with parameter of equivalent Gaussian PSF. This enables the analysis of motion and triangular blurs in terms of equivalent Gaussian PSF. This is a result of linear relationship between transformation of the parameters of these PSFs and corresponding transformation of parameter of the equivalent Gaussian PSF. In this case linear relationship between parameters allows us to use it on various analysis, which otherwise is not correct as described in [13]. We select blur PSF and corresponding parameters that control the blur spread in a manner such that the quality of the recovered image and amount of compression are optimized. We use deconvolution to recover the original image from the blurred image. Hence, PSFs with filter-coefficients of very small order such as Gaussian filters boost the errors and result in poor quality recovered image compared with filters with high-order coefficients like motion blur PSF.

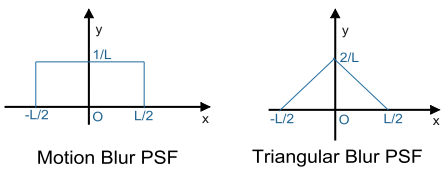

Figure 3. Motion blur PSF and triangular blur PSF.

Figure 4 shows the effect of choice of various blur PSFs on achieved compression through the proposed technique. We observe from the figure that the amount of compression increases with increase in blur parameter σ. For motion blur PSF, the σ represents the blur parameter of equivalent Gaussian kernel for the motion blur length L as described in Theorem 1. Similarly, σ for the triangular blur is related to width L as in Theorem 2. We also observe that larger support yields larger compression. We observe that the triangular blur PSF as well as Gaussian PSF achieves more compression than motion blur PSF for the same blur parameter σ due to larger support.

Figure 5 shows the effect of choice of various blur PSFs on PSNR of the recovered images from compressed images through the proposed compression technique. We observe that PSNR decreases with increase in blur parameter σ. We also observe that PSNR for the motion blur PSF is the highest among blur PSFs for the same blur parameter σ.

Figure 6 shows the effect of different blur PSFs on SSIM of the image recovered from compressed image obtained

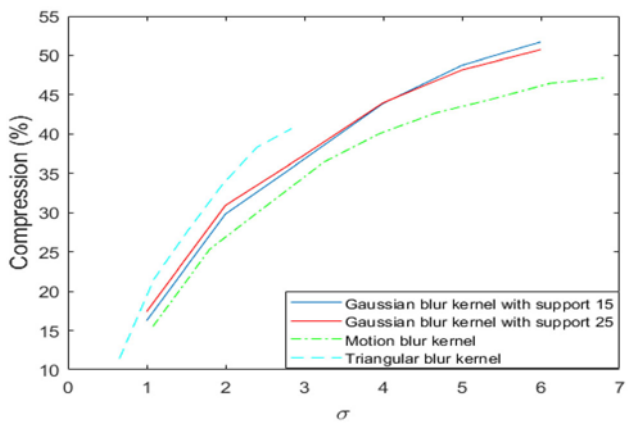

Figure 4. Effect of various blur PSFs on compression.

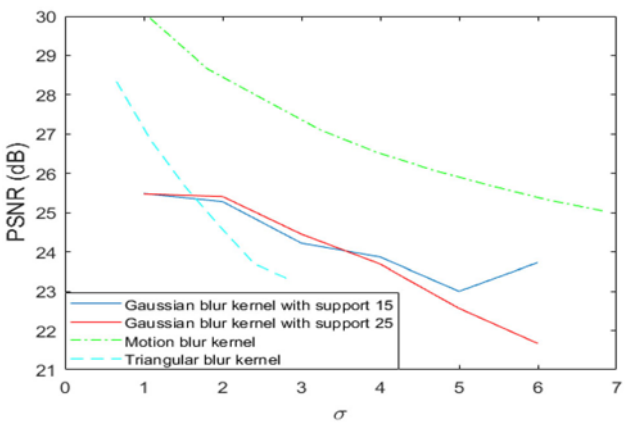

Figure 5. Effect of blur PSFs on PSNR.

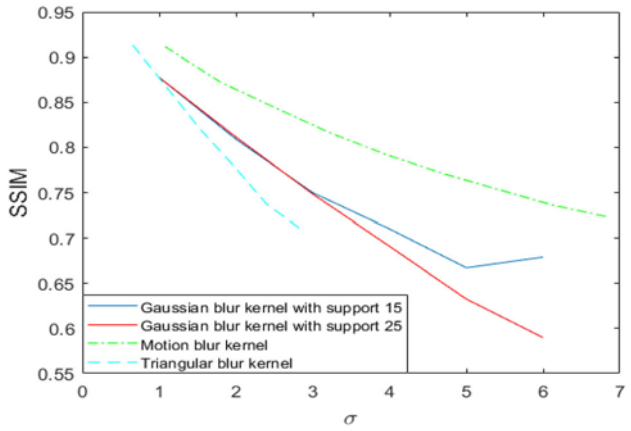

Figure 6. Effect of blur PSFs on SSIM.

using the proposed spectrum-based technique. We observe that SSIM decreases with increase in blur parameter σ. This happens due to deconvolution errors caused by quantization effects. We also observe that SSIM for the motion blur PSF is the highest for the same blur parameter σ.

Figures 4–6 show metrics for the proposed compression technique with different PSFs. The desired PSF along with parameters can be chosen according to maximum allowed tolerance in SSIM and PSNR. Usually, PSNR values greater than 30 and SSIM values greater than 80% are considered to be good quality.

4.3 *JPEG compression*

JPEG is a lossy compression technique [6] based on perceptual measure. The compression process is applied such that there is perceptually no observable difference in image quality. JPEG compression involves dividing the entire image into 8×8 blocks and applying DCT. We keep those DCT coefficients that satisfy perceptual measure requirement and neglect the rest. This yields overall compression in image encoding. We follow the reverse process for image decoding.

4.4 *Image recovery*

We recover the original image from the blurred image by deconvolution using selected blur PSF based on spectrum orientation. Blurring is a result of convolution of image with blur PSF. In case of finite impulse response, zeros of inputs are preserved in output; we call this property as 'zero preservation' as given in (11). Here, h is blur PSF, x is input and y is blurred output.

$$y = x * h \quad \Rightarrow \quad Y(z) = X(z)H(z). \tag{11}$$

Discarding boundary elements of the blurred output alters the zeros and thereby leads to inaccuracies in deconvolution. Thus, preservation of boundary elements in convolution output is desired to attain high deconvolution accuracy. Hence, we store the boundary elements of blurred output y to increase the deconvolution accuracy. We use Cho's method [24] for deblurring. This method has become a standard amongst deblurring methods due to its high accuracy and low time complexity.

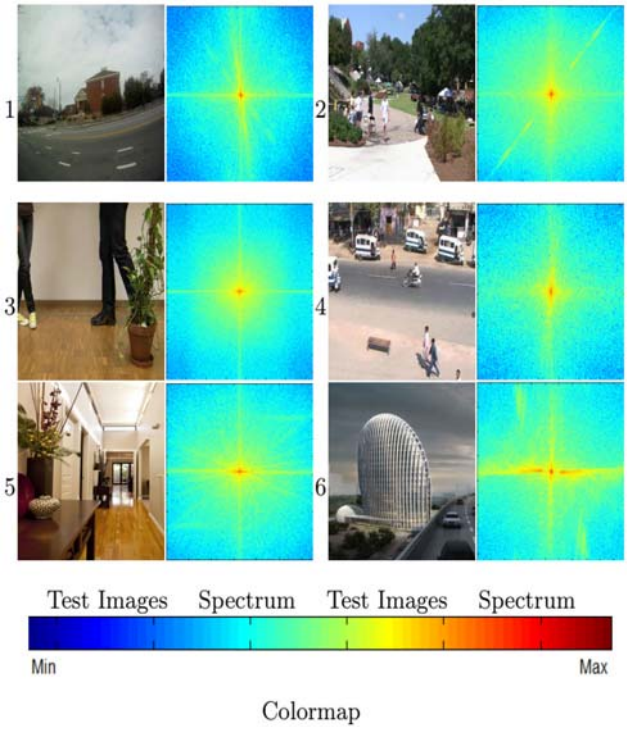

Figure 7. Test images and their corresponding spectra. Colormap shows the colour coding of the image spectrum.

5. Results

In this section, we present the results for proposed compression method. Our test environment contains MATLAB in Windows 10 environment in 'Intel(R) i3-3120M'

Table 1. Effect of PSF orientation on compression (over JPEG).

Image	PSF	$\angle S$	Compression(%)	PSNR (dB)	SSIM
1	h	90°	18	36	0.96
	v		30	35	0.94
2	h	45°	37	28	0.85
	v		37	28	0.85
3	h	invariant	25	37	0.94
	v		25	37	0.94
4	h	90°	27	28	0.90
	v		34	29	0.88
5	h	0°	31	32	0.93
	v		24	33	0.95
6	h	0°	32	28	0.93
	v		23	31	0.95

architecture. To verify the theory behind the proposed method, we applied compression using the proposed method on a few test images shown in Figure 7.

We observe from Figure 7 that the spectra of test images are an-isotropic. Thus, we select the blurring PSF for optimum compression as discussed in Section 4. We have selected motion blur PSF of length 9 as blurring kernel to obtain a reasonable SSIM along with good PSNR. The direction of blur PSF is determined from the orientation of frequency spectrum $\angle S$ as discussed in section 4.

Table 1 shows additional compression achieved over JPEG using the proposed method for different orientations of blur PSF for test images shown in Figure 7. Here h and v denote, respectively, horizontal and vertical blur PSFs. We observe from the Table that the proposed compression method achieves more than 25% compression over the standard JPEG compression, i.e. we achieve more than 25% compression with respect to original JPEG-compressed image. We also observe that choosing PSF orientation in the direction of spectrum orientation results in higher compression. We conclude that the proposed method can be employed to compress an image to reduce the data footprint.

Figure 8 shows the recovered images from the compressed images using the proposed method. We observe from the figure that the recovered images do not contain perceivable differences from original images barring some fringing effect at the border, which can be matted easily. This is also reflected in terms of high values of PSNR and SSIM for the recovered images as given in Table 1.

To verify the efficacy of the proposed method, we also performed the compression test over a large database. This database contains 4107 images collected from internet. Firstly, we estimated the spectrum orientation for the images in database and observed an interesting fact that the spectra of almost 67% images are DI as given in Table 2. Also, a very small fraction of images have spectrum oriented in horizontal direction. This signifies the fact that we can choose blurring PSF in vertical direction and obtain significant compression over a large set of images by reducing the processing further.

Table 2. Spectrum orientation prior.

	No. of images with $\angle S$ as		
No. of images	Direction invariant	0°	90°
4107	2751	246	1110

Table 3 shows the compression metrics for the collected database containing 4107 images. We have used motion blur PSF with blur length 9 as blurring PSF along with three cases of PSF orientation selection schemes, viz 'adaptive' as given in section 4.1, 'horizontal PSF' and 'vertical PSF'. We computed the compression metrics for images with 'DI' PSFs, images with horizontal 'HZ' PSFs and images with vertical 'V' PSFs. The Table also presents the average compression metrics 'Avg' for the entire database. We observe from the Table that the average compression metrics 'Avg' for all the PSF selection schemes are close due to spectrum orientation prior as given in Table 2. Thus, we can reduce the time complexity for the encoding by fixing the blur kernel as vertically oriented kernel.

Table 4 presents the compression results for two JPEG coding standards. We observe from the Table that the proposed technique achieves around 25% more compression compared with JPEG coding standard with high PSNR and SSIM. We also observe that the compression using JPEG2000 yields higher values of PSNR and SSIM with higher size of compressed output.

Processing time is another key factor for real time applications of proposed technique. Generally, 5 s is considered as an average time required for loading a webpage [25]. Figure 9 shows the time complexity of the proposed method for image recovery. We observe from the figure that the time complexity increases linearly with increase in image size. Processing time can be further reduced using parallelization of the deconvolution process.

Figure 8. Recovered image using proposed method. First row contains the original images and second row contains the corresponding recovered images.

Table 3. Effect of PSF orientation on compression. DI: direction invariant, HZ: horizontal, V: vertical.

	Compression (%)				PSNR (dB)				SSIM			
PSF Selection	DI	HZ	V	Avg	DI	HZ	V	Avg	DI	HZ	V	Avg
Adaptive	29.52	26.30	34.33	30.63	29.79	31.22	29.55	29.81	0.84	0.86	0.83	0.84
Horizontal PSF	27.11	26.30	25.30	26.57	29.88	31.22	30.19	30.04	0.85	0.86	0.86	0.85
Vertical PSF	29.52	17.89	34.33	30.12	29.79	32.19	29.55	29.87	0.84	0.89	0.83	0.84

Table 4. Performance comparison on standard test images for JPEG and JPEG2000 coding standard (size in kB).

		JPEG coding standard				JPEG2000 coding standard			
Image	Size (kB)	Size-JPEG (kB)	Size-proposed	PSNR (dB)	SSIM	Size-JPEG2000 (kB)	Size-proposed (kB)	PSNR (dB)	SSIM
Lena	769	37.79	26.03	29.45	0.7729	342	102	32.97	0.8639
Baboon	657	75.73	56.19	28.55	0.8511	258	138	32.31	0.9231
Peppers	281	23.51	18.75	30.22	0.8272	159	60	37.54	0.947
Boat	174	41.92	25.25	29.4	0.8224	152	62	31.91	0.8695
Cameraman	38	10.72	7.15	24.94	0.8744	35	18	31.1	0.9546
Barbara	240	40.69	22.73	26.8	0.7818	106	53	29.48	0.8556

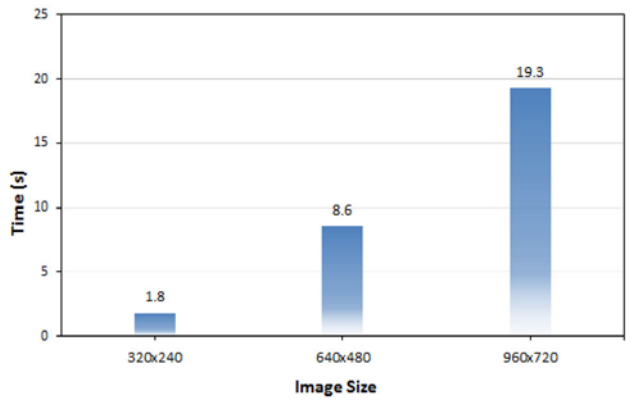

Figure 9. Computation time for the proposed method.

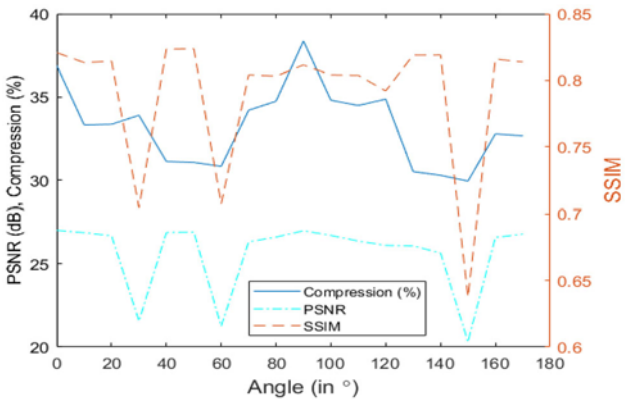

Figure 10. Effect of PSF orientation variation on compression metrics for the proposed method.

6. Discussion

In this paper, we have selected PSF only in 0° and 90° directions as discussed in subsection 4.1. The main reason behind such a selection is finite angle resolution due to digitization and quantization. The finite resolution results in spread of blur PSF coefficients for directions other than 0°, 45° and 90°. This, in turn, results in poor PSNR of the deconvolved output as discussed in subsection 4.2.

Figure 10 shows the effect of the orientation variation of PSF on the compression metrics, viz PSNR, SSIM and compression for a test image using the proposed method. We have used motion blur PSF with blur length 7 for this experiment. We observe from the figure that the quantization significantly affects the compression metrics. Thus, we select the blur PSF direction to be either 0° or 90° based on the dominant energy orientation.

7. Limitations

Accuracy of the proposed method depends on accuracy of deconvolution from quantized output. Fine textures and presence of noise may inversely affect the performance of

proposed method due to heavy quantization effect. However, one can choose smaller blurring PSF in such cases for the proposed method. In future, we would like to address this issue for obtaining high-quality deconvolved output. The proposed method utilizes computational resources to reduce the data footprint. In future, we would like to optimize the utilization of computational resources such that processing time for proposed method gets minimized. As discussed earlier, in principle, non-customary methods can be used simultaneously; however, errors in one method can severely affect the performance of other method. In future, we would like to combine non-customary methods such as Google's RAISR with the proposed method.

8. Conclusion

In this paper, we propose a novel method for image compression using blurring and deblurring of an image. The optimal blurring PSF is selected based on the spectrum of image. The main source of compression in proposed technique is reduced intensity variation among pixels due to blurring, which can be efficiently encoded by DCT. In this paper, we also present a framework to express parameters of different PSFs using a common parameter σ. This calibration enables us to compare the output obtained using different PSFs. This paper utilizes Gaussian function for the calibration of parameters of different PSFs. In future, we would like to further extend these concepts to obtain a generalized theory. The proposed technique is a non-customary method of compression and can be applied alongside other compression techniques. Techniques such as [20] can be used to represent colour image as grey scale image by hiding colour information in textured regions. As image compression techniques can also be applied for video compression, in future, we would like to extend the proposed method for the case of videos.

References

[1] David A Huffman 1952 A method for the construction of minimum-redundancy codes. *Proceedings of the IRE* 40: 1098–1101

[2] Rachit Patel, Sapna Katiyar and Khushboo Arora 2016 An improved image compression technique using Huffman coding and FFT. In: *Proceedings of the International Conference on Smart Trends for Information Technology and Computer Communications*. Springer, pp. 54–61

[3] Marco Conoscenti, Riccardo Coppola and Enrico Magli 2016 Constant SNR, rate control, and entropy coding for predictive lossy hyperspectral image compression. *IEEE Transactions on Geoscience and Remote Sensing* 54: 7431–7441

[4] Dacil Barreto, Alvarez L D, Rafael Molina, Aggelos K Katsaggelos and Callico G M 2007 Region-based super-resolution for compression. *Multidimensional Systems and Signal Processing* 18: 59–81

[5] Yaniv Romano, John Isidoro and Peyman Milanfar 2017 RAISR: rapid and accurate image super resolution. *IEEE Transactions on Computational Imaging* 3: 110–125

[6] Gregory K Wallace 1992 The JPEG still picture compression standard. *IEEE Transactions on Consumer Electronics* 38(1): xviii–xxxiv

[7] Awwal Mohammed Rufai, Gholamreza Anbarjafari and Hasan Demirel 2014 Lossy image compression using singular value decomposition and wavelet difference reduction. *Digital Signal Processing* 24: 117–123

[8] Mohammad H Asghari and Bahram Jalali 2014 Discrete anamorphic transform for image compression. *IEEE Signal Processing Letters* 21: 829–833

[9] Detlev Marpe and Hans L Cycon 1997 Efficient pre-coding techniques for wavelet-based image compression. *Proceedings of PCS* 97: 45–50

[10] Geoffrey M Davis 1998 A wavelet-based analysis of fractal image compression. *IEEE Transactions on Image Processing* 7(2): 141–154

[11] Kamrul Hasan Talukder and Koichi Harada 2010 Haar wavelet based approach for image compression and quality assessment of compressed image. *arXiv preprint arXiv:1010.4084*

[12] Himanshu Kumar, Sumana Gupta and Venkatesh K S 2017 A novel method for image compression using spectrum. In: *Proceedings of the Ninth International Conference on Advances in Pattern Recognition (ICAPR-2017)*. IEEE, pp. 1–6

[13] Himanshu Kumar, Sumana Gupta and Venkatesh K S 2019 Blur Parameter Locus Curve (BPLC) and its applications. *IET Image Processing* 14: 297–309

[14] Chao Dong, Chen Change Loy, Kaiming He and Xiaoou Tang 2016 Image super-resolution using deep convolutional networks. *IEEE Transactions on Pattern Analysis and Machine Intelligence* 38: 295–307

[15] George Toderici, Damien Vincent, Nick Johnston, Sung Jin Hwang, David Minnen, Joel Shor and Michele Covell 2016 Full resolution image compression with recurrent neural networks. *arXiv preprint arXiv:1608.05148*

[16] Michele Covell, Nick Johnston, David Minnen, Sung Jin Hwang, Joel Shor, Saurabh Singh, Damien Vincent and George Toderici 2017 Target-quality image compression with recurrent, convolutional neural networks. *arXiv preprint arXiv:1705.06687*

[17] Nick Johnston, Damien Vincent, David Minnen, Michele Covell, Saurabh Singh, Troy Chinen, Sung Jin Hwang, Joel Shor and George Toderici 2017 Improved lossy image compression with priming and spatially adaptive bit rates for recurrent networks. *arXiv preprint arXiv:1703.10114*

[18] Xinpeng Zhang 2011 Lossy compression and iterative reconstruction for encrypted image. *IEEE Transactions on Information Forensics and Security* 6: 53–58

[19] Akhtar N, Khan S and Siddiqui G April 2014 A novel lossy image compression method. IEEE, pp. 866–870

[20] Sambuddha Kumar and Sumana Gupta 2014 Color video compression using color mapping into textured grayscale video frames. *Pattern Analysis and Applications* 17: 809–822

[21] Nanrun Zhou, Yixian Wang, Lihua Gong, Hong He and Jianhua Wu 2011 Novel single-channel color image encryption algorithm based on chaos and fractional Fourier transform. *Optics Communications* 284: 2789–2796

[22] Liansheng Sui and Bo Gao 2013 Single-channel color image encryption based on iterative fractional Fourier transform and chaos. *Optics & Laser Technology* 48: 117–127

[23] Brendt Wohlberg 2016 Convolutional sparse representation of color images. In: *Proceedings of the 2016 IEEE Southwest Symposium on Image Analysis and Interpretation (SSIAI)*. IEEE, pp. 57–60

[24] Sunghyun Cho and Seungyong Lee 2009 Fast motion deblurring. *ACM Transactions on Graphics* 28: 145

[25] Ahmad Bakeri Abu Baka and Nur Leyni 2017 Webometric study of world class universities websites. *Qualitative and quantitative methods in libraries*, pp. 105–115